

## Gene therapy rescues cone function in congenital achromatopsia

András M. Komáromy<sup>1,\*</sup>, John J. Alexander<sup>2,3,4</sup>, Jessica S. Rowlan<sup>1</sup>, Monique M. Garcia<sup>1,5</sup>,  
Vince A. Chiodo<sup>3</sup>, Asli Kaya<sup>5</sup>, Jacqueline C. Tanaka<sup>5</sup>, Gregory M. Acland<sup>6</sup>, William W.  
Hauswirth<sup>2,3</sup> and Gustavo D. Aguirre<sup>1</sup>

<sup>1</sup>Department of Clinical Studies, School of Veterinary Medicine, University of Pennsylvania, Philadelphia, PA 19104, USA, <sup>2</sup>Department of Molecular Genetics and Microbiology, University of Florida, Gainesville, FL 32610, USA, <sup>3</sup>Department of Ophthalmology and Powell Gene Therapy Center, University of Florida, Gainesville, FL 32610, USA, <sup>4</sup>Vision Science Research Center, University of Alabama, Birmingham, AL 35294, USA, <sup>5</sup>Department of Biology, Temple University, Philadelphia, PA 19122, USA and <sup>6</sup>Baker Institute, Cornell University, Ithaca, NY 14853, USA

\*To whom correspondence should be addressed at: Department of Clinical Studies, School of Veterinary Medicine, University of Pennsylvania, 3900 Delancey Street, Philadelphia, PA 19104-6010, USA. Tel: +1 2155732695; Fax: +1 2155732162; Email: komaromy@vet.upenn.edu.

## ABSTRACT

The successful restoration of visual function with recombinant adeno-associated virus (rAAV)-mediated gene replacement therapy in animals and humans with an inherited disease of the retinal pigment epithelium has ushered in a new era of retinal therapeutics. For many retinal disorders, however, targeting of therapeutic vectors to mutant rods and/or cones will be required. In this study, the primary cone photoreceptor disorder achromatopsia served as the ideal translational model to develop gene therapy directed to cone photoreceptors. We demonstrate that rAAV-mediated gene replacement therapy with different forms of the human red cone opsin promoter led to the restoration of cone function and day vision in 2 canine models of *CNGB3* achromatopsia, a neuronal channelopathy that is the most common form of achromatopsia in man. The robustness and stability of the observed treatment effect was mutation-independent but promoter- and age-dependent. Subretinal administration of rAAV5-*hCNGB3* with a long version of the red cone opsin promoter in younger animals led to a stable therapeutic effect for at least 33 months. Our results hold promise for future clinical trials of cone-directed gene therapy in achromatopsia and other cone-specific disorders.

## INTRODUCTION

Most vision impairing disorders in humans result from genetic defects, and, to date, mutations have been identified in ~150 genes out of ~200 mapped retinal disease loci (RetNet: <http://www.sph.uth.tmc.edu/RetNet/>). This wealth of genetic information has provided fundamental understanding of the multiple and specialized roles played by photoreceptors and the retinal pigment epithelium (RPE) in the visual process, and how mutations in these genes result in disease. Together with the development of gene transfer technologies, it is now possible to realistically consider the use of gene therapy to treat these previously untreatable disorders. A new era of retinal therapeutics has been started by recent studies showing that treatment of animal models with gene therapy successfully restored visual function (1-3). These results have been translated to the clinic and been shown to be safe and successful for a human retinal degeneration caused by *RPE65* mutations (4-11).

However, this example of an RPE disease is rare and complex in that loss of visual function and eventual photoreceptor degeneration is secondary to a biochemical blockade of the RPE visual cycle. While it has been an ideal test platform for the first clinical gene therapy trial for blindness in man, *RPE65* disease is not representative of the diversity of more common retinal disorders that could be considered for gene therapy where the target cells are the rods and/or cones. For these, successful targeting of therapeutic vectors to mutant photoreceptors to restore function and preserve structure will be required, and achieving this initially in experimental animals is necessary for eventual application to humans.

Congenital achromatopsia, also called rod monochromacy or total congenital color blindness, is a rare autosomal recessive disorder with an estimated prevalence of about 1 in 30,000 - 50,000 (12-15). Because it primarily affects cones, it serves as the ideal translational model to develop

gene therapies directed to photoreceptors. Even though cones are numerically small, ~ 5% of the photoreceptors in man (16), they are essential for color vision, central visual acuity and most daily visual activities, functions that are severely impaired or absent in affected patients. Thus far, 4 genes have been identified to cause achromatopsia in human patients, all of them encoding principal components of the cone phototransduction cascade: the *alpha* subunit of cone transducin (GNAT2) (17-19), the catalytic *alpha*' subunit of the cone phosphodiesterase (PDE6C) (20,21), and the *alpha* (CNGA3) (22-24) and *beta* (CNGB3) (25-28) subunits of the cone cyclic nucleotide-gated (CNG) channel located in the plasma membrane of the cone outer segment. The majority of human achromatopsia (~70 - 92%) are considered channelopathies as they are caused by mutations in either *CNGA3* or *CNGB3* (29-32). The *CNGB3* gene appears to be the most prevalent causal gene for achromatopsia in patients of Northern European descent, with reported prevalences between 50 and 87% (29,32). However, it is suspected that *CNGA3* mutations are more prevalent among patients from the Middle East (33).

Based on the very high prevalence of the *CNGB3* mutations in autosomal recessive achromatopsia (29,32), our identification of two independent canine models with distinct *CNGB3* mutations has provided us with a unique, physiologically relevant system in which to assess potential gene therapy strategies designed to restore visual function (34). These models result from either a missense mutation in exon 6 (*CNGB3<sup>m/m</sup>*) or a genomic deletion of the entire *CNGB3* gene (*CNGB3<sup>-/-</sup>*, "null mutation") (34). The canine disease caused by the null mutation has been characterized, and shares the same clinical phenotype as human patients (35-38). The classic achromatopsia phenotype develops between 8 and 12 weeks of age, soon after retinal differentiation is completed (35-38); however, other than the salient functional and structural abnormalities in affected cones, the retina remains normal throughout life (36,38).

Here we report the successful restoration of cone function and associated photopic vision in both canine achromatopsia models by gene replacement therapy. We used recombinant adeno-associated virus serotype 5 (rAAV5) with different forms of the human red cone opsin promoter. The robustness and stability of the observed treatment effect was mutation-independent but promoter- and age-dependent. These results hold promise for future clinical trials in human patients with *CNGB3*-achromatopsia.

## RESULTS

### **Cones are present but not functional in canine *CNGB3*-achromatopsia**

In contrast to man and nonhuman primates that have separate populations of red, green and blue cones, dogs are functional dichromats, with cone populations having combined red/green and blue pigments (39). These are termed long/medium-wavelength-absorbing cones (L/M-cones) and short-wavelength-absorbing cones (S-cones), and have maximal sensitivities of 555 nm and 429 - 435 nm, respectively (39,40). The number, distribution and ratios of L/M- and S-cones in the normal canine retina has recently been reported, and L/M-cones outnumber S-cones by a ratio of 8:1 in the areas selected for therapy (see Materials and Methods) (41).

Dogs with either the *CNGB3*<sup>-/-</sup> or *CNGB3*<sup>m/m</sup> mutation are blind in bright light after ~8 weeks of age, a time point when vision can be reproducibly evaluated (35-38,42). At this age cone-mediated function is absent, but rod responses are normal (Fig. 1). Despite the loss of cone function, both L/M- and S-cones are present, and express markers characteristic of their differentiated state (Fig. 2). Cone arrestin is expressed in both L/M- and S-cones, but expression in the outer segments appears to be more intense in the former (Fig. 2). Although there has been quantification of the rate of cone loss in canine *CNGB3*-achromatopsia with time (unpublished

data), we find that the process is slow with many cones still present in older affected dogs (Supplementary Material, Fig. S1). Thus the time window for cone-targeted gene replacement therapy deserves examination.

### **Gene expression can be targeted to cones in *CNGB3*-achromatopsia by rAAV**

In an effort to direct treatment to cones, we first asked whether mutant cones could be transduced with vectors conveying reporter constructs and promoters that are derived from L/M-cones. We previously reported the effectiveness and specificity of rAAV5 and different versions of the human red cone opsin promoter to direct cell class-specific GFP expression to L/M-cones in normal and diseased (primary, early rod degeneration caused by *PDE6B* mutation) canine retina (43). In preparation for rAAV5-mediated gene replacement therapy in *CNGB3*-achromatopsia, we confirmed that the longer (PR2.1) and shorter (3LCR-PR0.5) variants of the human red cone opsin promoter were also able to target L/M-cones in mutant canine retinas (Table 1). We found that gene expression could be targeted specifically to non-functional L/M-cones in the *CNGB3*-mutant retina, and that the robustness of expression was promoter-dependent. While the PR2.1 led to strong GFP expression that could be easily visualized by direct GFP fluorescence, expression with the shorter 3LCR-PR0.5 promoter was weaker, and required immunohistochemical enhancement to visualize the transduced cones (Fig. 3). We also verified that the transfection of cones only occurred in the area of the subretinal bleb, and that GFP-gene expression levels diminished sharply beyond the bleb margins (Fig. 3). Both PR2.1 and 3LCR-PR0.5 promoters were subsequently used for rAAV5-mediated gene replacement therapies. The shortest version of the human red cone opsin promoter PR0.5 was not evaluated with the GFP reporter gene in *CNGB3*-mutant retinas, but was tested in the therapeutic studies. We did not

attempt to use the human blue cone opsin promoter because we previously found that expression was promiscuous, with GFP present in few L/M-cones, some rods, and RPE, but not S-cones (43).

### **rAAV-mediated gene replacement therapy restores cone function**

A single subretinal injection of rAAV5 vector containing the human *CNGB3* (*hCNGB3*) transgene restored cone function in *CNGB3*-mutant dogs as measured by cone flicker ERG (Fig. 1). In dogs maintained for long-term follow up, the rescued cone function was sustained for well over 1 year with the longest period of observation being ~2.5 years (130 weeks), suggesting that the correction is stable and likely permanent (Table 1 and Fig. 4). This successful treatment outcome was mutation-independent, but promoter- and age-dependent (Table 2), and there was no difference in treatment outcomes between the *CNGB3*<sup>m/m</sup> and the *CNGB3*<sup>-/-</sup> animals.

Efficient and sustained cone function rescue could not be achieved with vectors containing the two shorter promoters, PR0.5 and 3LCR-PR0.5. Despite undetectable GFP expression in canine cones with the shortest human red cone opsin promoter PR0.5 (43), it resulted in transient restoration of cone function in 1 of 2 injected eyes (Table 2). Using the more robust 3LCR-PR0.5 promoter (43), 2 of 7 injected eyes showed transient restoration of cone function (Table 2). In the eyes responding to the injections with either of the shorter promoters, recordable ERG cone function was present at 3 weeks after therapy, but was lost by 13 weeks. In contrast, the longest promoter, PR2.1, provided robust and stable rescue of cone function in 12 of 17 eyes (Table 2); once rescue of cone function was achieved, it was sustained.

In addition to promoter effectiveness, we studied the age-dependence on functional cone rescue. Even though many cones are still present in affected older dogs several years of age

(Supplementary Material, Fig. S1), we observed that only 1 of 3 eyes of dogs over 54 weeks of age showed a clear restoration of cone function when treated with vector having the PR2.1 promoter. In contrast 11 out of 14 eyes responded when treatment was done in eyes less than 28 weeks of age (Table 2). Similar outcomes were observed with the two other shorter human red cone opsin promoters although the number of animals evaluated in each group was smaller.

In addition to not having found rescue of function following the application of GFP vectors, we ruled out a sham treatment effect by injecting 10 eyes of 8 dogs (5 *CNGB3*<sup>-/-</sup> and 3 *CNGB3*<sup>m/m</sup>) between 4 and 76 weeks of age subretinally with comparable volumes of the vector excipient balanced salt solution (BSS, Alcon Laboratories, Inc., Fort Worth, TX). Cone function was not restored in any of these animals (data not shown), an indication that return of cone function was entirely dependent on the presence of the *hCNGB3* transgene in the vector.

### **rAAV-mediated gene replacement therapy restores photopic vision**

In addition to the electrophysiologic documentation of cone-function recovery, qualitative and quantitative vision testing was performed on selected dogs following gene therapy. Initially vision under bright-light conditions was assessed subjectively by observing the dogs maneuver around randomly placed obstacles in a confined area. Untreated dogs showed clear signs of day-blindness including hypermetric gait, disorientation and collision with obstacles, while treated dogs were sighted (Supplementary Material, Movie S1). All animals exhibited no visual deficits in a dim light environment.

To assess visual function in a more quantifiable and objective manner, 7 affected dogs, 6 treated with PR2.1-*hCNGB3* and one with PR0.5-*hCNGB3*, had their visual function tested objectively under scotopic and photopic conditions in an obstacle avoidance course. Objective



identification of achromatopsia was based on transit time, a quantitative response variable (42). There was a significant increase in mean transit times of achromatopsia-affected dogs in ambient light intensities of  $\geq 25$  lux, while the mean transit times of normal control dogs were not affected by any ambient light conditions (Fig. 5). In contrast, following gene therapy in affected dogs, transit times under photopic conditions approached normal values, but were still slower. This remaining difference between normal and treated affected dogs is expected given that normal dogs function binocularly in the obstacle course, while the treated dogs received the vector injection in only one eye. Additionally, only approximately 30% of the retina was treated. Given these differences, the behavioral similarities between normal and treated dogs are remarkable. Performance in the obstacle course is illustrated in Movie S2 (Supplementary Material).

### **Normalization of protein localization accompanies rAAV-mediated rescue of cone function**

To more fully assess rescue of the cone phenotype, the expression and localization of cone *alpha* transducin GNAT2 and CNGA3 proteins was evaluated by immunohistochemistry. In the normal retina, both GNAT2 and CNGA3 were found in the cone outer segments. In contrast, the non-functional cones in the *CNGB3*<sup>-/-</sup> and *CNGB3*<sup>m/m</sup> retinas did not have either GNAT2 or CNGA3 in the outer segments (Fig. 6), but western blot analysis demonstrated that the CNGA3 protein was present in the retina (Fig. 6). This was previously reported for other transducin subunits in the canine *CNGB3*<sup>-/-</sup> retina (44,45). At all time points evaluated, the examination of successfully treated retinal regions showed restoration of protein localization to cone outer segments for both GNAT2 and CNGA3 associated with rescued function (Fig. 6). This was limited to the vector treated area and not visible in untreated regions (data not shown). We interpret these findings to indicate that successful restoration of cone function was accompanied by relocation of CNG

channel components and transducin, both elements of the phototransduction cascade, to their proper cone outer segment compartment.

### **A minimum level of transgene expression is necessary but not sufficient to restore cone function**

All the retinas analyzed at various times following subretinal rAAV5-*hCNGB3* injection showed expression of the *hCNGB3* transgene as measured by quantitative real-time PCR (qRT-PCR) (Fig. 7). The robustness of transgene expression with the PR2.1 promoter confirmed our previous findings using reporter GFP expression with this promoter (43). For comparison we also measured mRNA levels of canine *CNGB3* (*cCNGB3*), *S-opsin*, *L/M-opsin*, and *rod opsin* relative to the 18S rRNA endogenous control. In treated eyes that did not show recovery of cone-function, the *hCNGB3*-transgene expression was lower, by ~ 3.6 - 150 fold compared to successfully treated eyes, but clearly still detectable (Fig. 7). This means that *hCNGB3* transgene expression must exceed a threshold level to be sufficient to restore cone function. As expected, expression of *cCNGB3* mRNA was not present in null mutant dogs, but was comparable to wildtype animals in the missense mutant dogs (Fig. 7). When we compared the detectable retinal *hCNGB3* transgene expression levels with the cone flicker ERG amplitudes measured before tissue collection, we found a highly significant nonparametric Spearman rank correlation of 0.85 ( $p < 0.0001$ ); that is, cone ERG flicker amplitude increased with higher *hCNGB3* transgene expression (Fig. 7).

## DISCUSSION

We report that gene replacement therapy restores retinal cone function in 2 canine models of *CNGB3* achromatopsia, a neuronal channelopathy. Restored cone function was documented by cone specific ERG and recovery of day vision. As mutations in *CNGB3* are the most common cause of achromatopsia in humans, our results hold promise for future clinical trials. We also showed that the restoration of cone function is mutation-independent, but promoter- and age-dependent. Using vectors with the PR2.1 promoter, phenotypic correction is stable and likely permanent.

Results with vectored GFP reporter gene in mutant retinas confirmed that cones are present despite total lack of function after 8 weeks of age, and that gene expression can be selectively targeted to them. We previously showed the specificity and robustness of some human red cone opsin promoters, the shorter 3LCR-PR0.5 and the more robust longer PR2.1, to target GFP reporter gene expression to normal canine cones (43). The same 2 promoters allowed us to also target the non-functional cones in the 2 strains of *CNGB3*-mutant dogs with the same robustness as in normals. We also confirmed that transgene expression is limited to the area of the subretinal bleb, and then gradually fades beyond the treatment borders (43,46,47). In contrast to the high efficiency and specificity obtained with the human red cone opsin promoters, we have not been able to target canine S-cones with the currently available human S-cone promoter (43). Work in several species has showed that S-cones can be targeted, but with low specificity (48-51). Even though optimizing targeting to all classes of cones would be desirable from a therapeutic perspective, S-cones represent the minority in both dogs (9 - 12% of the total cone population (41)), and most other mammalian species including human and non-human primates (52,53).

Thus significant clinical improvement of quality of life and vision can be expected even with restoration of only M- and L-cone function.

The robustness of GFP expression observed with each promoter matched the outcome of rescued cone function, i.e. the highest success rate with the longest lasting treatment effect was achieved with the longest promoter, PR2.1. The shorter 3LCR-PR0.5 promoter also resulted in recordable restored cone function, but with a much smaller success rate and only transiently. Use of the shortest promoter, PR0.5, resulted in transient restoration of cone function even though we could not detect any expression of *GFP* reporter gene in normal dogs (43). We do not have a clear explanation for the transient treatment effect observed with the shorter promoters other than postulating an initial peak in *hCNGB3* transgene expression which then decreased below a therapeutic threshold. This would be reflected in longitudinal changes in expression during the first few weeks after subretinal injection, but such a study has not been done yet. A trophic factor response to the insult of the subretinal injection is not likely as we have not found such an effect in the *GFP*-vector and balanced salt solution (BSS) injected eyes.

The level of *hCNGB3* transgene expression significantly differed between retinas that were successfully treated with the PR2.1 promoter and retinas that only transiently responded with the 3LCR-PR0.5 promoter. The importance of transgene expression levels is further supported by its significant correlation with cone flicker ERG amplitudes. What remains unclear is the minimum level needed to restore function. Several animals that failed to respond to the treatment with the longer PR2.1 promoter still showed levels of expression close to those with rescued cone function. In order to gain clarity about some of these questions, transgene expression should be monitored over time to determine its kinetics and to compare it to the timeline of rescued cone function and recovery of day vision. Because none of the therapeutic failures could be explained

solely by lack of transgene expression, other factors may also determine the restoration of cone function, e.g. the synthesis of CNGB3 protein in sufficient quantities and the proper assembly of the CNGA3 and CNGB3 protein subunits into a functional tetrameric outer segment channel (54). As well, there was no observable retinal damage that could have explained a failed therapeutic effect despite detectable *hCNGB3* transgene expression.

In addition to promoter effects, we also observed a reproducible reduction in the cone therapy success rate in dogs treated at 54 weeks of age or older. The underlying molecular mechanism for this phenomenon remains to be determined, particularly in view of the fact that many cones that appear structurally normal are still present in older animals. We have not observed such an age-effect in our previous work on rAAV-mediated gene therapy in dogs with Leber Congenital Amaurosis caused by *RPE65*-mutation (*RPE65*-LCA) (55). One possibility is that it may result from the greater complexity of interacting phototransduction elements in photoreceptors, either rods or cones, in comparison to those of the retinoid cycle in the RPE. This might suggest that a return to "normal" following gene replacement therapy in photoreceptors requires more protein reorganization than it does for comparable therapy in the RPE. This issue may have a potential impact on the age of patients initially selected for an achromatopsia gene therapy clinical trial.

We have not observed a detrimental effect of potential *hCNGB3* transgene overexpression, which probably occurred with the PR2.1 promoter, on the cone photoreceptors, particularly in missense mutant dogs. One can imagine that too many CNG channels on the cone outer segment membrane may negatively affect the cones. However, CNG channels are heterotetramers that are composed of homologous *alpha* and *beta* subunits (CNGA3 and CNGB3 in cones) (56,57), and

it is possible that the number of CNG channels in the cone outer segment membrane is determined primarily by the expression levels of *CNGA3* rather than *CNGB3*.

Our results represent the second successful cone-directed gene replacement therapy in achromatopsia animal models; the first being rAAV-mediated gene therapy of the *GNAT2*<sup>cpfl3</sup> mutant mouse (58). The value of our results lies in the fact that the achromatopsia dogs represent the only natural large animal model of *CNGB3*-achromatopsia, the most common form of the disease in man (29,32). Furthermore, the canine disease is unlike some of the naturally occurring or experimental mouse achromatopsia models which are characterized by early and rapid cone cell loss (59,60). The *CNGB3* mutant dog retina shows normal development and preservation of cones, and degeneration and loss occur slowly, thus increasing the therapeutic time window.

We documented the successful gene therapy in the *CNGB3*-mutant dogs by the restoration of both the cone ERG and by objective measure of day vision behavior. The behavioral results suggest that inner retinal cells and central visual pathways were able to usefully process the input from the recovered cones, at least within the ages treated. The cortical effects of the functional deficit, however, are not clear at present, and are important areas for further studies of translational significance. That visual cortical plasticity occurs in response to changes in peripheral inputs has been described in recent work in the mouse and squirrel monkey where inner retinal cells and central visual pathways are able to adjust an additional cone cell class (61,62). Achromatopsia studies in man have shown a large-scale reorganization of the visual cortex in which the cortical region that normally responds to signals from the all-cone foveola, and is inactive in normal subjects under rod viewing conditions, becomes highly responsive to rod-initiated signals (63). One possibility is that restoration of central cone function in such patients would result in remapping of the visual cortex, although such studies would need to be

carried out only after confirming cone ERG restoration upon treatment. Even though dogs lack a foveo-macular region, they are an excellent model to examine cortical plasticity upon vector treatment as shown by the functional cortical imaging methods being currently developed (55) using "silent substitution methods" that are able to separate rod vs cone, and S-cone vs L/M-cone cortical responses (64).

In conclusion, robust, long-term rescue of cone function was achieved in 2 canine models of *CNGB3*-achromatopsia. As mutations in *CNGB3* are the most common cause of human achromatopsia, studies on a corresponding natural disease in dogs offer unique opportunities for proof-of-principle experiments examining cone-directed gene therapy for eventual translation to patients. Because cones are also compromised in many other retinal diseases, e.g. cone dystrophies (21,22), or cone-rod dystrophies (65,66), and secondarily in many forms of age-related macular degeneration (AMD) (67,68) and retinitis pigmentosa (69-71), results reported here offer a promise for future cone-directed gene therapy in humans.

## MATERIALS AND METHODS

### Animals

A total of 33 achromatopsia affected dogs were studied, both males and females, between 3 and 81 weeks of age. These had either a genomic deletion (*CNGB3*<sup>-/-</sup>; n = 24) or a missense mutation (*CNGB3*<sup>m/m</sup>; n = 9) of the *CNGB3* gene (Table 1) (34). The animals were part of a research colony maintained at the Retinal Disease Studies Facility (Kennett Square, PA, USA) and supported by the National Eye Institute, NIH (EY-06855), and a Foundation Fighting Blindness Center grant. For terminal procedures, the dogs were euthanized with an overdose of sodium pentobarbital, and the eyes enucleated for molecular and protein studies and

immunohistochemistry. All procedures in this study were approved by the University of Pennsylvania IACUC, and were done in accordance with the ARVO Statement for the Use of Animals in Ophthalmic and Vision Research.

## Vectors

Recombinant adeno-associated virus vectors of serotype 5 (rAAV5) were used. The vector constructs with the green fluorescent protein (*GFP*) reporter gene have recently been described (43). The *CNGB3* therapeutic vectors were constructed similarly with the *hCNGB3* cDNA replacing the GFP coding sequence. Promoter constructs were based on the same red-cone opsin promoter derived from the pR2.1-LacZ plasmid containing bases spanning -4564 to -3009 and -496 to 0 of the human red cone pigment gene driving LacZ (49). Briefly, the vector plasmid pTR-PR2.1-*Gnat2* was digested with *NotI* to release the murine *Gnat2* gene, and the *NotI* linearized pTR-PR2.1 backbone was isolated. A plasmid containing the human *CNGB3* gene (2430bp) was used as a template for a PCR reaction with primers (forward 5' – TTTGCGGCCGCAATGTTTAAATCGCTGACAAAAGTCA – 3' and reverse 5' – TTTGCGGCCGCTTATTGCTTAGCCTTTTCTTTGACT – 3') to introduce *NotI* sites 5' and 3' of the ATG start and TAA stop codons, respectively, of *CNGB3*. The *CNGB3* PCR product was sub-cloned into a pCR-Blunt vector, digested with *NotI*, isolated, and cloned into the pTR-PR2.1 backbone to create the vector plasmid pTR-PR2.1-*hCNGB3*. The vector plasmid also contains an SV40 Poly-A tail located 3' of the stop codon. The rAAV constructs for PR0.5 and 3LCR PR0.5 driving *hCNGB3* were created in a similar manner. Briefly, only the “core” -496 to 0 promoter sequence was used for PR0.5, and three copies of the 37bp locus control region fused to the upstream sequence of the core promoter was used for 3LCR-PR0.5. SURE cells



(Stratagene, La Jolla, CA) were used to propagate all rAAV constructs. The final sequence for the *hCNGB3* gene used in our study differed from the published sequence in two places: (1) at +540 were an A to G at the third position in the codon resulted in a silent mutation (Pro to Pro) and (2) at +892 where an A to C at the first position in the codon resulted in a missense mutation (Thr to Pro), a known polymorphism in the gene (28). Production and purification of rAAV5 was carried out by procedures similar to those previously described (72,73). Quantitative real-time PCR (qRT-PCR) was used to determine titer, and the final rAAV5 aliquots in balanced salt solution (BSS, Alcon Laboratories, Inc., Fort Worth, TX) with 0.014% Tween 20 were stored at -80 °C.

### Vector administration

Subretinal administration of vector containing either a reporter or therapeutic gene was performed in 25 dogs (*CNGB3*<sup>-/-</sup>, n = 19; *CNGB3*<sup>m/m</sup>, n = 6) ranging in age from 3 - 81 weeks of age with a RetinaJect™ subretinal injector (SurModics, Inc., Eden Prairie, MN) through a transvitreal approach under general anesthesia using methods previously described (43,74). The majority of dogs had unilateral injections, and the fellow eye served as control. In all cases, the area treated was in the tapetal zone superior to the optic disc, a region with very high cone density (41). Because eye size changes dramatically with age, and there are limits to the volume that can be delivered to the subretinal space, vector volumes were chosen so that most of this region was covered; these ranged between 60 and 190 μL. Vector concentrations varied somewhat in different production lots, but most were in the range of 10<sup>12</sup> vector genomes (vg)/mL. In order to rule out a sham treatment effect by the subretinal injection alone, ten eyes of 8 dogs (5 *CNGB3*<sup>-/-</sup> and 3 *CNGB3*<sup>m/m</sup>) aged between 4 and 76 weeks were injected with

comparable volumes of BSS. Immediately following surgery, the retinal location and extent of the subretinal blebs were documented by fundus drawings for reference in the morphologic studies. Details of the injections and experimental procedures performed in animals receiving either the therapeutic or reporter gene constructs are summarized in Table 1.

Post-operative management included a combination of subconjunctival steroids, topical antibiotic-steroids and mydriatics, and short term systemic steroids and antibiotics as previously described (43,74). Using this protocol, the uveitis induced by the surgical trauma remained mild, and no signs of ocular pain or periocular swelling were noticed. Following surgery, the dogs were monitored by routine ophthalmic examination with binocular indirect ophthalmoscopy and slitlamp biomicroscopy. Flattening of the subretinal bleb occurred within 24 - 36 hours. In general, the surgical procedure and vectors were well tolerated. Expected side effects were limited to mild anterior and posterior uveitis immediately after subretinal injection that was easily controlled with the routine medical management (43,74). In 3 of the 17 eyes injected with the rAAV5-PR2.1-*hCNGB3* vector a multifocal chorioretinitis developed between 3 and 5 weeks post injection. This abnormality only developed at higher vector concentrations, was easily controlled with systemic steroid treatment and no longer occurred when vector doses were lowered. Long-term we found variable degrees of retinal scarring in the region of the retinotomy site; these changes have been documented before (75). However, 4 animals injected with a particular rAAV5 vector lot developed severe, sterile, endophthalmitis within 12 - 24 hours subretinal injection due to endotoxin contamination of the vector preparation. These animals were not included in this report, and the problem has been resolved by additional purification steps.

## **Electroretinography**

Standard Ganzfeld scotopic (dark-adapted) and photopic (light-adapted) electroretinograms (ERGs) were obtained from anesthetized dogs using a modified Ganzfeld dome fitted with the LED light stimuli transferred from a ColorDome stimulator (Diagnosys LLC, Lowell, MA). The ERGs were recorded with custom-built Burian-Allen bipolar contact lens electrodes (Hansen Labs, Coralville, IA), commercially available platinum subdermal needle electrodes (Grass Safelead Needle electrodes; Grass Technologies, Astro-Med, Inc., West Warwick, RI), and the Espion E<sup>2</sup> computer based system (Diagnosys LLC). Following premedication (acepromazine maleate, 0.5 mg/kg SQ; atropine sulfate, 0.03 mg/kg SQ) and intravenous thiobarbiturate induction (thiopental sodium, 25 mg/kg), the dogs were maintained under isoflurane inhalation anesthesia for the ERG recordings. The procedures for electroretinography setup were standard and have been reported previously (76,77). Rod and mixed cone-rod mediated responses were recorded after 20 minutes of dark-adaptation with scotopic single white flash stimuli of increasing intensities (from 0.000577 to 10.26 cd.sec/m<sup>2</sup>). Following 10 minutes of light-adaptation to a background illumination of 34.26 cd/m<sup>2</sup>, 1-Hz single flash (from 0.00577 to 10.26 cd.sec/m<sup>2</sup>) and 29.41-Hz flicker (from 0.00577 to 5.77 cd.sec/m<sup>2</sup>) cone mediated signals were recorded. Except for the brighter scotopic light stimuli ( $\geq 0.577$  cd.sec/m<sup>2</sup>) multiple responses were averaged.

## **Objective vision testing**

To complement the retinal functional studies, we developed an obstacle course that provides an objective assessment of visual performance in dogs under variable scotopic and photopic conditions. Details of the apparatus and testing method have been described (42). The testing is

comparable to that used in human patients in one of the *RPE65* clinical trials (PAMELA-Pedestrian Accessibility and Movement Environment Laboratory (7)). With this testing modality we can reliably and reproducibly distinguish affected achromatopsia dogs from normal dogs because of their significantly longer transit time through the course at light intensities  $\geq 25$  lux (42). For every dog the averaged transit time from 3 trials at each of the 4 illuminance levels was used for data analysis. Comparisons of mean transit times between groups were conducted using a generalized linear model, which adjusts the correlation from repeated measures at various illuminance levels in the same dog.

### **Retinal morphology and immunohistochemistry**

Following enucleation, the eyes were fixed for 3 hours in 4% paraformaldehyde in 0.1 M PBS at 4 °C, and processed for embedding in optimal cutting temperature (OCT) medium as previously described (78). Using the fundus drawings made immediately following subretinal injection and in the clinical examinations done post-treatment, the globes were oriented prior to trimming so that treated and untreated regions of the eye were included for evaluation in the same retinal sections. Ten  $\mu\text{m}$  cryosections were cut and examined for intrinsic GFP fluorescence, immunohistochemistry or after H&E staining to examine retinal morphology and assess any adverse effects of the treatment.

For eyes injected with a *GFP*-vector, green fluorescence was first evaluated in unstained sections using a Zeiss Axioplan microscope (Carl Zeiss Meditec GmbH, Oberkochen, Germany) with epifluorescence illumination (Filter Set 23 with GFP excitation at 489 nm and emission at 509 nm). Those sections with absent or weak green fluorescence were labeled with a GFP polyclonal antibody (rabbit 1:1,000). Immunohistochemical staining was performed using S-

opsin polyclonal antibody (rabbit 1:5,000; Chemicon, Millipore, Billerica, MA; or goat 1:50; Santa Cruz Biotechnology, Inc., Santa Cruz, CA), L/M-opsin polyclonal antibody (rabbit 1:100; Chemicon; or goat 1:100; Santa Cruz), cone *alpha* transducin (rabbit 1:5,000; Santa Cruz), human cone arrestin (rabbit 1:10,000), and canine CNGA3 (rabbit 1:5,000). The latter polyclonal antibody was generated in rabbits against the carboxyl terminal peptide of canine CNGA3 (NH<sub>2</sub>-GIPGDAAKTEIKEQ-COOH) and affinity purified. Alexa Fluor® labeled goat anti-rabbit IgG or donkey anti-goat IgG (1:200; Molecular Probes, Inc., Eugene, OR) was used as secondary antibody. DAPI stain was used to detect cell nuclei. Images were digitally captured (Spot 4.0 camera; Diagnostic Instruments, Inc., Sterling Heights, MI), and imported into a graphics program (Photoshop; Adobe Systems, Inc., San Jose, CA) for display. An antibody against canine CNGB3 is not available presently. Five prior attempts to produce antibodies against CNGB3 peptides (n=4) or protein (n=1) have not been successful, and antibodies available to CNGB3 of mouse and human are not specific in the dog.

### **Quantitative real-time PCR analysis of retinal transgene expression**

Whole retinas were isolated from the eyecups within 1 - 2 minutes of death, flash frozen in liquid nitrogen, and stored at -80°C until used. The retinal tissue was homogenized, and total RNA extracted with TRIzol Reagent (Invitrogen, Carlsbad, CA) extraction. RNA concentrations were determined using a ND1000 Nanodrop spectrophotometer (NanoDrop Products, Wilmington, DE). Retinal cDNA was synthesized by reverse transcription using the High Capacity cDNA Reverse Transcription kit (Applied Biosystems, Carlsbad, CA) and the manufacturer's instructions. Primers and TaqMan® MGB™ probes were designed for the *hCNGB3* transgene, canine *CNGA3* (*cCNGA3*), *cCNGB3*, *L/M-opsin*, *S-opsin*, and *rod opsin* using Primer Express

Software Version 2.0 (Applied Biosystems) (Supplementary Material, Table S1). To ensure that only cDNA and not genomic DNA was amplified, primer pairs were designed to neighboring exon sequences. Eukaryotic 18S rRNA was used as an endogenous control (Hs99999901\_s1; Applied Biosystems). Quantitative RT-PCR was conducted with TaqMan® Gene Expression Mastermix (Applied Biosystems) using an ABI 7500 Real Time PCR System (Applied Biosystems). Each reaction was run in quadruplicate, and contained 50 ng of cDNA template along with 900 nM forward and reverse primers for each gene in a final reaction volume of 30  $\mu$ l. PCR cycling parameters were 50°C for 2 minutes, then 95°C for 10 minutes, followed by 40 cycles of 95°C for 15 seconds, with a final step of 60°C for 1 minute. Relative gene expression for each gene compared to the 18S rRNA product was calculated as  $1 / [2^{(Ct_{Gene} - Ct_{18S})}]$  and compared for each gene among dog groups by one-way analysis of variance. Expression of the *hCNGB3* transgene was compared to the 29-Hz flicker amplitudes by nonparametric Spearman rank correlation.

### **Western blotting**

Retinas were harvested as described for qRT-PCR analysis and frozen at -80°C. Each retina was homogenized with 5 strokes on ice in 0.5 ml of RIPA buffer (1% Triton X-100, 1% sodium deoxycholate, 0.1% SDS, 158mM NaCl, 10mM Tris) containing protease inhibitor cocktail (Sigma-Aldrich Corp., St. Louis, MO). The homogenate was centrifuged for 10 minutes at 4°C at 14,000 rpm. Forty  $\mu$ g of protein was loaded onto each lane. For comparison, cultured tSA-203 cells were transfected with 1.5  $\mu$ g of canine CNGA3 cDNA and cell extracts prepared as described previously (79). The primary cCNGA3 antibody was diluted at 1:500 and detected with ECL™ horseradish peroxidase-conjugated secondary anti-rabbit antibody (GE Healthcare

Biosciences, Pittsburgh, PA) diluted to 1:1,000. For the housekeeping protein primary polyclonal *beta* actin antibody (rabbit; Abcam, Inc., Cambridge, MA) was diluted 1:1,000 and the secondary anti-rabbit antibody 1:5,000. Immunoreactivity was visualized using Amersham ECL™ Western Blotting Detection Reagents (GE Healthcare).

## FUNDING

This work was supported by the National Institutes of Health [K12-EY015398 to A.M.K. (PI: Maureen G. Maguire), R01-EY019304 to A.M.K., R01-EY013132 to G.D.A., R01-EY006855 to G.M.A., T32-EY007132 to W.W.H., P30-EY008571 to W.W.H., R01-EY011123 to W.W.H., R01-EY017549 to G.D.A., and P30-EY001583 (NEI Core Grant to the University of Pennsylvania; PI: David H. Brainard)]; the Foundation Fighting Blindness (Center grant to G.D.A.); the Macula Vision Research Foundation (to W.W.H.); the McCabe Fund (to A.M.K.); the ONCE International Prize (to G.D.A.); the Van Sloun Fund for Canine Genetic Research (to G.D.A.); and an unrestricted gift from Brittany Rockefeller and family (to G.D.A. and A.M.K.).

## ACKNOWLEDGEMENTS

We thank Jeremy Nathans (Johns Hopkins University – Howard Hughes Medical Institute) for the pR2.1-LacZ plasmid; Bernd Wissinger (University Clinics Tübingen) for the *hCNGB3* cDNA; W. Clay Smith (University of Florida) for the GFP antibody; Cheryl M. Craft (University of Southern California) for the hCAR antibody; and Tom Doyle and Min Ding (University of Florida) for assistance in vector production. We also thank Ann Cooper, Amanda Nickle, Gerri Antonini, Alice Eidsen, Tracy Greiner, Sanford Boye, Gui-shuang Ying, Jason Hinmon, and the staff of the Retinal Disease Studies Facility at the University of Pennsylvania for technical

support, and Mary Leonard for excellent illustrations. We thank Paul A. Sieving (National Eye Institute) for encouraging one of the investigators (A.M.K.) to enter the retinal research field.

*Conflict of Interest statement.* W.W.H. and the University of Florida have a financial interest in the use of rAAV therapies, and own equity in a company (AGTC Inc.) that may commercialize some aspects of this work. University of Pennsylvania, University of Florida and Cornell University hold a patent on the described gene therapy technology (United States Patent 20070077228, “Method for Treating or Retarding the Development of Blindness”). All remaining authors have declared that no conflict of interest exists.



## REFERENCES

1. Acland,G.M., Aguirre,G.D., Ray,J., Zhang,Q., Aleman,T.S., Cideciyan,A.V., Pearce-Kelling,S.E., Anand,V., Zeng,Y., Maguire,A.M. *et al.* (2001) Gene therapy restores vision in a canine model of childhood blindness. *Nat. Genet.*, **28**, 92-95.
2. Acland,G.M., Aguirre,G.D., Bennett,J., Aleman,T.S., Cideciyan,A.V., Bennicelli,J., Dejneka,N.S., Pearce-Kelling,S.E., Maguire,A.M., Palczewski,K. *et al.* (2005) Long-term restoration of rod and cone vision by single dose rAAV-mediated gene transfer to the retina in a canine model of childhood blindness. *Mol. Ther.*, **12**, 1072-1082.
3. Pang,J.J., Chang,B., Kumar,A., Nusinowitz,S., Noorwez,S.M., Li,J., Rani,A., Foster,T.C., Chiodo,V.A., Doyle,T. *et al.* (2006) Gene therapy restores vision-dependent behavior as well as retinal structure and function in a mouse model of *RPE65* Leber congenital amaurosis. *Mol. Ther.*, **13**, 565-572.
4. Hauswirth,W.W., Aleman,T.S., Kaushal,S., Cideciyan,A.V., Schwartz,S.B., Wang,L., Conlon,T.J., Boye,S.L., Flotte,T.R., Byrne,B.J. *et al.* (2008) Treatment of Leber congenital amaurosis due to *RPE65* mutations by ocular subretinal injection of adeno-associated virus gene vector: Short-term results of a phase I trial. *Hum. Gene Ther.*, **19**, 979-990.
5. Cideciyan,A.V., Aleman,T.S., Boye,S.L., Schwartz,S.B., Kaushal,S., Roman,A.J., Pang,J.J., Sumaroka,A., Windsor,E.A., Wilson,J.M. *et al.* (2008) Human gene therapy for RPE65 isomerase deficiency activates the retinoid cycle of vision but with slow rod kinetics. *Proc. Natl. Acad. Sci. U. S. A.*, **105**, 15112-15117.
6. Maguire,A.M., Simonelli,F., Pierce,E.A., Pugh,E.N.,Jr, Mingozzi,F., Bennicelli,J., Banfi,S., Marshall,K.A., Testa,F., Surace,E.M. *et al.* (2008) Safety and efficacy of gene transfer for Leber's congenital amaurosis. *N. Engl. J. Med.*, **358**, 2240-2248.

7. Bainbridge, J.W., Smith, A.J., Barker, S.S., Robbie, S., Henderson, R., Balaggan, K., Viswanathan, A., Holder, G.E., Stockman, A., Tyler, N. *et al.* (2008) Effect of gene therapy on visual function in Leber's congenital amaurosis. *N. Engl. J. Med.*, **358**, 2231-2239.
8. Cideciyan, A.V., Hauswirth, W.W., Aleman, T.S., Kaushal, S., Schwartz, S.B., Boye, S.L., Windsor, E.A., Conlon, T.J., Sumaroka, A., Roman, A.J. *et al.* (2009) Vision 1 year after gene therapy for Leber's congenital amaurosis. *N. Engl. J. Med.*, **361**, 725-727.
9. Cideciyan, A.V., Hauswirth, W.W., Aleman, T.S., Kaushal, S., Schwartz, S.B., Boye, S.L., Windsor, E.A., Conlon, T.J., Sumaroka, A., Pang, J.J. *et al.* (2009) Human *RPE65* gene therapy for Leber congenital amaurosis: Persistence of early visual improvements and safety at 1 year. *Hum. Gene Ther.*, **20**, 999-1004.
10. Maguire, A.M., High, K.A., Auricchio, A., Wright, J.F., Pierce, E.A., Testa, F., Mingozzi, F., Benniselli, J.L., Ying, G.S., Rossi, S. *et al.* (2009) Age-dependent effects of *RPE65* gene therapy for Leber's congenital amaurosis: A phase 1 dose-escalation trial. *Lancet*, **374**, 1597-1605.
11. Simonelli, F., Maguire, A.M., Testa, F., Pierce, E.A., Mingozzi, F., Benniselli, J.L., Rossi, S., Marshall, K., Banfi, S., Surace, E.M. *et al.* (2010) Gene therapy for Leber's congenital amaurosis is safe and effective through 1.5 years after vector administration. *Mol. Ther.*, **18**, 643-650.
12. Sharpe, L.T. and Nordby, K. (1990) Total Colour Blindness: An Introduction. In Hess R.F., Sharpe L.T. and Nordby K. (eds.), *Night Vision: Basic, Clinical and Applied Aspects*. Cambridge University Press, Cambridge, pp. 253-289.
13. Michaelides, M., Hunt, D.M. and Moore, A.T. (2004) The cone dysfunction syndromes. *Br. J. Ophthalmol.*, **88**, 291-297.

14. Michaelides, M., Hardcastle, A.J., Hunt, D.M. and Moore, A.T. (2006) Progressive cone and cone-rod dystrophies: Phenotypes and underlying molecular genetic basis. *Surv. Ophthalmol.*, **51**, 232-258.
15. Simunovic, M.P. and Moore, A.T. (1998) The cone dystrophies. *Eye (Lond)*, **12 ( Pt 3b)**, 553-565.
16. Curcio, C.A., Sloan, K.R., Kalina, R.E. and Henrickson, A.E. (1990) Human photoreceptor topography. *J. Comp. Neurol.*, **292**, 497-523.
17. Kohl, S., Baumann, B., Rosenberg, T., Kellner, U., Lorenz, B., Vadala, M., Jacobson, S.G. and Wissinger, B. (2002) Mutations in the cone photoreceptor G-protein alpha-subunit gene GNAT2 in patients with achromatopsia. *Am. J. Hum. Genet.*, **71**, 422-425.
18. Aligianis, I.A., Forshew, T., Johnson, S., Michaelides, M., Johnson, C.A., Trembath, R.C., Hunt, D.M., Moore, A.T. and Maher, E.R. (2002) Mapping of a novel locus for achromatopsia (ACHM4) to 1p and identification of a germline mutation in the alpha subunit of cone transducin (GNAT2). *J. Med. Genet.*, **39**, 656-660.
19. Rosenberg, T., Baumann, B., Kohl, S., Zrenner, E., Jorgensen, A.L. and Wissinger, B. (2004) Variant phenotypes of incomplete achromatopsia in two cousins with GNAT2 gene mutations. *Invest. Ophthalmol. Vis. Sci.*, **45**, 4256-4262.
20. Chang, B., Grau, T., Dangel, S., Hurd, R., Jurklies, B., Sener, E.C., Andreasson, S., Dollfus, H., Baumann, B., Bolz, S. *et al.* (2009) A homologous genetic basis of the murine cpfl1 mutant and human achromatopsia linked to mutations in the PDE6C gene. *Proc. Natl. Acad. Sci. U. S. A.*, **106**, 19581-19586.
21. Thiadens, A.A., den Hollander, A.I., Roosing, S., Nabuurs, S.B., Zekveld-Vroon, R.C., Collin, R.W., De Baere, E., Koenekoop, R.K., van Schooneveld, M.J., Strom, T.M. *et al.* (2009)

- Homozygosity mapping reveals *PDE6C* mutations in patients with early-onset cone photoreceptor disorders. *Am. J. Hum. Genet.*, **85**, 240-247.
22. Wissinger,B., Gamer,D., Jagle,H., Giorda,R., Marx,T., Mayer,S., Tippmann,S., Broghammer,M., Jurklies,B., Rosenberg,T. *et al.* (2001) *CNGA3* mutations in hereditary cone photoreceptor disorders. *Am. J. Hum. Genet.*, **69**, 722-737.
23. Kohl,S., Marx,T., Giddings,I., Jagle,H., Jacobson,S.G., Apfelstedt-Sylla,E., Zrenner,E., Sharpe,L.T. and Wissinger,B. (1998) Total colourblindness is caused by mutations in the gene encoding the *alpha*-subunit of the cone photoreceptor cGMP-gated cation channel. *Nat. Genet.*, **19**, 257-259.
24. Wissinger,B., Jagle,H., Kohl,S., Broghammer,M., Baumann,B., Hanna,D.B., Hedels,C., Apfelstedt-Sylla,E., Randazzo,G., Jacobson,S.G. *et al.* (1998) Human rod monochromacy: Linkage analysis and mapping of a cone photoreceptor expressed candidate gene on chromosome 2q11. *Genomics*, **51**, 325-331.
25. Sundin,O.H., Yang,J.M., Li,Y., Zhu,D., Hurd,J.N., Mitchell,T.N., Silva,E.D. and Maumenee,I.H. (2000) Genetic basis of total colourblindness among the Pingelapese islanders. *Nat. Genet.*, **25**, 289-293.
26. Winick,J.D., Blundell,M.L., Galke,B.L., Salam,A.A., Leal,S.M. and Karayiorgou,M. (1999) Homozygosity mapping of the achromatopsia locus in the pingelapese. *Am. J. Hum. Genet.*, **64**, 1679-1685.
27. Milunsky,A., Huang,X.L., Milunsky,J., DeStefano,A. and Baldwin,C.T. (1999) A locus for autosomal recessive achromatopsia on human chromosome 8q. *Clin. Genet.*, **56**, 82-85.
28. Kohl,S., Baumann,B., Broghammer,M., Jagle,H., Sieving,P., Kellner,U., Spegal,R., Anastasi,M., Zrenner,E., Sharpe,L.T. *et al.* (2000) Mutations in the *CNGB3* gene encoding

- the *beta*-subunit of the cone photoreceptor cGMP-gated channel are responsible for achromatopsia (ACHM3) linked to chromosome 8q21. *Hum. Mol. Genet.*, **9**, 2107-2116.
29. Kohl,S., Varsanyi,B., Antunes,G.A., Baumann,B., Hoyng,C.B., Jagle,H., Rosenberg,T., Kellner,U., Lorenz,B., Salati,R. *et al.* (2005) *CNGB3* mutations account for 50% of all cases with autosomal recessive achromatopsia. *Eur. J. Hum. Genet.*, **13**, 302-308.
  30. Varsanyi,B., Wissinger,B., Kohl,S., Koeppen,K. and Farkas,A. (2005) Clinical and genetic features of hungarian achromatopsia patients. *Mol. Vis.*, **11**, 996-1001.
  31. Wiszniewski,W., Lewis,R.A. and Lupski,J.R. (2007) Achromatopsia: The *CNGB3* p.T383fsX mutation results from a founder effect and is responsible for the visual phenotype in the original report of uniparental disomy 14. *Hum. Genet.*, **121**, 433-439.
  32. Thiadens,A.A., Slingerland,N.W., Roosing,S., van Schooneveld,M.J., van Lith-Verhoeven,J.J., van Moll-Ramirez,N., van den Born,L.I., Hoyng,C.B., Cremers,F.P. and Klaver,C.C. (2009) Genetic etiology and clinical consequences of complete and incomplete achromatopsia. *Ophthalmology*, **116**, 1984-1989.e1.
  33. Ahuja,Y., Kohl,S. and Traboulsi,E.I. (2008) *CNGA3* mutations in two United Arab Emirates families with achromatopsia. *Mol. Vis.*, **14**, 1293-1297.
  34. Sidjanin,D.J., Lowe,J.K., McElwee,J.L., Milne,B.S., Phippen,T.M., Sargan,D.R., Aguirre,G.D., Acland,G.M. and Ostrander,E.A. (2002) Canine *CNGB3* mutations establish cone degeneration as orthologous to the human achromatopsia locus ACHM3. *Hum. Mol. Genet.*, **11**, 1823-1833.
  35. Aguirre,G.D. and Rubbin,L.F. (1975) The electroretinogram in dogs with inherited cone degeneration. *Invest. Ophthalmol.*, **14**, 840-847.

36. Aguirre,G.D. and Rubin,L.F. (1974) Pathology of hemeralopia in the Alaskan malamute dog. *Invest. Ophthalmol.*, **13**, 231-235.
37. Rubin,L.F. (1971) Hemeralopia in Alaskan malamute pups. *J. Am. Vet. Med. Assoc.*, **158**, 1699-1701.
38. Rubin,L.F. (1971) Clinical features of hemeralopia in the adult Alaskan malamute. *J. Am. Vet. Med. Assoc.*, **158**, 1696-1698.
39. Jacobs,G.H., Deegan,J.F.,2nd, Crognale,M.A. and Fenwick,J.A. (1993) Photopigments of dogs and foxes and their implications for canid vision. *Vis. Neurosci.*, **10**, 173-180.
40. Neitz,J., Geist,T. and Jacobs,G.H. (1989) Color vision in the dog. *Vis. Neurosci.*, **3**, 119-125.
41. Mowat,F.M., Petersen-Jones,S.M., Williamson,H., Williams,D.L., Luthert,P.J., Ali,R.R. and Bainbridge,J.W. (2008) Topographical characterization of cone photoreceptors and the area centralis of the canine retina. *Mol. Vis.*, **14**, 2518-2527.
42. Garcia,M.M., Ying,G.S., Cocomes,C.A., Tanaka,J.C. and Komaromy,A.M. (2010) Evaluation of a behavioral method for objective vision testing and identification of achromatopsia in dogs. *Am. J. Vet. Res.*, **71**, 97-102.
43. Komaromy,A.M., Alexander,J.J., Cooper,A.E., Chiodo,V.A., Glushakova,L.G., Acland,G.M., Hauswirth,W.W. and Aguirre,G.D. (2008) Targeting gene expression to cones with human cone opsin promoters in recombinant AAV. *Gene Ther.*, **15**, 1049-1055.
44. Gropp,K.E., Szel,A., Huang,J.C., Acland,G.M., Farber,D.B. and Aguirre,G.D. (1996) Selective absence of cone outer segment *beta* 3-transducin immunoreactivity in hereditary cone degeneration (cd). *Exp. Eye Res.*, **63**, 285-296.

45. Akhmedov,N.B., Piriev,N.I., Pearce-Kelling,S., Acland,G.M., Aguirre,G.D. and Farber,D.B. (1998) Canine cone transducin-*gamma* gene and cone degeneration in the cd dog. *Invest. Ophthalmol. Vis. Sci.*, **39**, 1775-1781.
46. Le Meur,G., Weber,M., Pereon,Y., Mendes-Madeira,A., Nivard,D., Deschamps,J.Y., Moullier,P. and Rolling,F. (2005) Postsurgical assessment and long-term safety of recombinant adeno-associated virus-mediated gene transfer into the retinas of dogs and primates. *Arch. Ophthalmol.*, **123**, 500-506.
47. Weber,M., Rabinowitz,J., Provost,N., Conrath,H., Folliot,S., Briot,D., Cherel,Y., Chenuaud,P., Samulski,J., Moullier,P. *et al.* (2003) Recombinant adeno-associated virus serotype 4 mediates unique and exclusive long-term transduction of retinal pigmented epithelium in rat, dog, and nonhuman primate after subretinal delivery. *Mol. Ther.*, **7**, 774-781.
48. Glushakova,L.G., Timmers,A.M., Pang,J., Teusner,J.T. and Hauswirth,W.W. (2006) Human blue-opsin promoter preferentially targets reporter gene expression to rat s-cone photoreceptors. *Invest. Ophthalmol. Vis. Sci.*, **47**, 3505-3513.
49. Wang,Y., Macke,J.P., Merbs,S.L., Zack,D.J., Klaunberg,B., Bennett,J., Gearhart,J. and Nathans,J. (1992) A locus control region adjacent to the human red and green visual pigment genes. *Neuron*, **9**, 429-440.
50. Khani,S.C., Pawlyk,B.S., Bulgakov,O.V., Kasperek,E., Young,J.E., Adamian,M., Sun,X., Smith,A.J., Ali,R.R. and Li,T. (2007) AAV-mediated expression targeting of rod and cone photoreceptors with a human rhodopsin kinase promoter. *Invest. Ophthalmol. Vis. Sci.*, **48**, 3954-3961.

51. Mauck,M.C., Mancuso,K., Kuchenbecker,J.A., Connor,T.B., Hauswirth,W.W., Neitz,J. and Neitz,M. (2008) Longitudinal evaluation of expression of virally delivered transgenes in gerbil cone photoreceptors. *Vis. Neurosci.*, **25**, 273-282.
52. Curcio,C.A., Allen,K.A., Sloan,K.R., Lerea,C.L., Hurley,J.B., Klock,I.B. and Milam,A.H. (1991) Distribution and morphology of human cone photoreceptors stained with anti-blue opsin. *J. Comp. Neurol.*, **312**, 610-624.
53. Roorda,A., Metha,A.B., Lennie,P. and Williams,D.R. (2001) Packing arrangement of the three cone classes in primate retina. *Vision Res.*, **41**, 1291-1306.
54. Peng,C., Rich,E.D. and Varnum,M.D. (2004) Subunit configuration of heteromeric cone cyclic nucleotide-gated channels. *Neuron*, **42**, 401-410.
55. Aguirre,G.K., Komaromy,A.M., Cideciyan,A.V., Brainard,D.H., Aleman,T.S., Roman,A.J., Avants,B.B., Gee,J.C., Korczykowski,M., Hauswirth,W.W. *et al.* (2007) Canine and human visual cortex intact and responsive despite early retinal blindness from *RPE65* mutation. *PLoS Med.*, **4**, e230.
56. Bonigk,W., Altenhofen,W., Muller,F., Dose,A., Illing,M., Molday,R.S. and Kaupp,U.B. (1993) Rod and cone photoreceptor cells express distinct genes for cGMP-gated channels. *Neuron*, **10**, 865-877.
57. Gerstner,A., Zong,X., Hofmann,F. and Biel,M. (2000) Molecular cloning and functional characterization of a new modulatory cyclic nucleotide-gated channel subunit from mouse retina. *J. Neurosci.*, **20**, 1324-1332.
58. Alexander,J.J., Umino,Y., Everhart,D., Chang,B., Min,S.H., Li,Q., Timmers,A.M., Hawes,N.L., Pang,J.J., Barlow,R.B. *et al.* (2007) Restoration of cone vision in a mouse model of achromatopsia. *Nat. Med.*, **13**, 685-687.



59. Michalakis,S., Geiger,H., Haverkamp,S., Hofmann,F., Gerstner,A. and Biel,M. (2005) Impaired opsin targeting and cone photoreceptor migration in the retina of mice lacking the cyclic nucleotide-gated channel CNGA3. *Invest. Ophthalmol. Vis. Sci.*, **46**, 1516-1524.
60. Ding,X.Q., Harry,C.S., Umino,Y., Matveev,A.V., Fliesler,S.J. and Barlow,R.B. (2009) Impaired cone function and cone degeneration resulting from CNGB3 deficiency: Down-regulation of CNGA3 biosynthesis as a potential mechanism. *Hum. Mol. Genet.*, **18**, 4770-4780.
61. Jacobs,G.H., Williams,G.A., Cahill,H. and Nathans,J. (2007) Emergence of novel color vision in mice engineered to express a human cone photopigment. *Science*, **315**, 1723-1725.
62. Mancuso,K., Hauswirth,W.W., Li,Q., Connor,T.B., Kuchenbecker,J.A., Mauck,M.C., Neitz,J. and Neitz,M. (2009) Gene therapy for red-green colour blindness in adult primates. *Nature*, **461**, 784-787.
63. Baseler,H.A., Brewer,A.A., Sharpe,L.T., Morland,A.B., Jagle,H. and Wandell,B.A. (2002) Reorganization of human cortical maps caused by inherited photoreceptor abnormalities. *Nat. Neurosci.*, **5**, 364-370.
64. Estevez,O. and Spekreijse,H. (1982) The "silent substitution" method in visual research. *Vision Res.*, **22**, 681-691.
65. Mears,A.J., Hiriyanna,S., Vervoort,R., Yashar,B., Gieser,L., Fahrner,S., Daiger,S.P., Heckenlively,J.R., Sieving,P.A., Wright,A.F. *et al.* (2000) Remapping of the RP15 locus for X-linked cone-rod degeneration to Xp11.4-p21.1, and identification of a *de novo* insertion in the *RPGR* exon ORF15. *Am. J. Hum. Genet.*, **67**, 1000-1003.

66. Fishman,G.A., Stone,E.M., Eliason,D.A., Taylor,C.M., Lindeman,M. and Derlacki,D.J. (2003) *ABCA4* gene sequence variations in patients with autosomal recessive cone-rod dystrophy. *Arch. Ophthalmol.*, **121**, 851-855.
67. Curcio,C.A., Medeiros,N.E. and Millican,C.L. (1996) Photoreceptor loss in age-related macular degeneration. *Invest. Ophthalmol. Vis. Sci.*, **37**, 1236-1249.
68. Phipps,J.A., Guymer,R.H. and Vingrys,A.J. (2003) Loss of cone function in age-related maculopathy. *Invest. Ophthalmol. Vis. Sci.*, **44**, 2277-2283.
69. Rosenfeld,P.J., Cowley,G.S., McGee,T.L., Sandberg,M.A., Berson,E.L. and Dryja,T.P. (1992) A null mutation in the *rhodopsin* gene causes rod photoreceptor dysfunction and autosomal recessive retinitis pigmentosa. *Nat. Genet.*, **1**, 209-213.
70. McLaughlin,M.E., Sandberg,M.A., Berson,E.L. and Dryja,T.P. (1993) Recessive mutations in the gene encoding the *beta*-subunit of rod phosphodiesterase in patients with retinitis pigmentosa. *Nat. Genet.*, **4**, 130-134.
71. Kajiwar,K., Berson,E.L. and Dryja,T.P. (1994) Digenic retinitis pigmentosa due to mutations at the unlinked *peripherin/RDS* and *ROM1* loci. *Science*, **264**, 1604-1608.
72. Zolotukhin,S. (2005) Production of recombinant adeno-associated virus vectors. *Hum. Gene Ther.*, **16**, 551-557.
73. Zolotukhin,S., Potter,M., Zolotukhin,I., Sakai,Y., Loiler,S., Fraites,T.J.,Jr, Chiodo,V.A., Phillipsberg,T., Muzyczka,N., Hauswirth,W.W. *et al.* (2002) Production and purification of serotype 1, 2, and 5 recombinant adeno-associated viral vectors. *Methods*, **28**, 158-167.
74. Komaromy,A.M., Varner,S.E., de Juan,E., Acland,G.M. and Aguirre,G.D. (2006) Application of a new subretinal injection device in the dog. *Cell Transplant.*, **15**, 511-519.

75. Jacobson,S.G., Acland,G.M., Aguirre,G.D., Aleman,T.S., Schwartz,S.B., Cideciyan,A.V., Zeiss,C.J., Komaromy,A.M., Kaushal,S., Roman,A.J. *et al.* (2006) Safety of recombinant adeno-associated virus type 2-*RPE65* vector delivered by ocular subretinal injection. *Mol. Ther.*, **13**, 1074-1084.
76. Acland,G.M. and Aguirre,G.D. (1987) Retinal degenerations in the dog: IV. Early retinal degeneration (erd) in Norwegian elkhounds. *Exp. Eye Res.*, **44**, 491-521.
77. Acland,G.M., Ray,K., Mellersh,C.S., Langston,A.A., Rine,J., Ostrander,E.A. and Aguirre,G.D. (1999) A novel retinal degeneration locus identified by linkage and comparative mapping of canine early retinal degeneration. *Genomics*, **59**, 134-142.
78. Beltran,W.A., Hammond,P., Acland,G.M. and Aguirre,G.D. (2006) A frameshift mutation in *RPGR* exon ORF15 causes photoreceptor degeneration and inner retina remodeling in a model of X-linked retinitis pigmentosa. *Invest. Ophthalmol. Vis. Sci.*, **47**, 1669-1681.
79. Patel,K.A., Bartoli,K.M., Fandino,R.A., Ngatchou,A.N., Woch,G., Carey,J. and Tanaka,J.C. (2005) Transmembrane S1 mutations in *CNGA3* from achromatopsia 2 patients cause loss of function and impaired cellular trafficking of the cone CNG channel. *Invest. Ophthalmol. Vis. Sci.*, **46**, 2282-2290.

## LEGENDS TO FIGURES

**Figure 1.** Normal rod function and loss of cone function in *CNGB3<sup>m/m</sup>*- and *CNGB3<sup>-/-</sup>*-mutant dogs and short-term restoration of cone ERG signals following a single subretinal treatment with rAAV5-PR2.1-*hCNGB3*. Representative, ERG traces evoked by full-field white flashes under dark-adapted (rod and mixed cone-rod responses) and light-adapted (cone 1 Hz and 29 Hz) conditions are shown. Compared to an age-matched normal wildtype dog the treated eye of the *CNGB3<sup>-/-</sup>* dog (M606; see Table 1) showed restoration of cone function as elicited by single and 29-Hz flicker light flashes 7 weeks after subretinal injection. The smaller amplitude of the restored cone function compared to the normal dog can be explained by the fact that the subretinal bleb covered ~30% of the entire retina.

**Figure 2.** Presence of L/M- and S-cones in *CNGB3*-mutant canine retinas, expressing markers that characterize the differentiated state. Comparison of canine retinal structure and cone-specific protein expression in normal (A1 – A4; 12 weeks), *CNGB3<sup>-/-</sup>* (B1 – B4; 17 weeks), and *CNGB3<sup>m/m</sup>* (C1 – C4; 12 weeks) dogs. The H&E-stained sections show normal outer retinal structure independent of disease status (A1, B1, C1). The expression and distribution of L/M- and S-opsin is not affected by the *CNGB3*-mutation. L/M-opsin labeling (green) co-localizes with cone arrestin expression (hCAR labeling in red) in the outer segments of the L/M-cones (A2, B2, C2). In contrast, cone arrestin labeling is weak in S-cone outer segments; hence the co-localized signal is dominated by the green S-opsin labeling (A3, B3, C3). Closer analysis of cone arrestin distribution shows that the hCAR labeling is much weaker in the S-cone outer segments compared to the L/M-cones of the canine wt retina (arrows in A4). hCAR labeling is essentially

not visible in the S-cone outer segments of the *CNGB3*-mutant dogs (arrows in B4 and C4).

Calibration bars = 20  $\mu\text{m}$ .

RPE, retinal pigment epithelium; OS, outer segment; IS, inner segment.

**Figure 3.** Promoter-dependent robustness of GFP-transgene expression in *CNGB3*<sup>-/-</sup>-mutant cone photoreceptors. (A) 25 weeks after subretinal injection, GFP expression is cone-specific, but weak when using the 3LCR-PR0.5 promoter; only one GFP-positive cone is seen without immunohistochemical labeling. (B) 38 weeks following injection with 3LCR-PR0.5 promoter, immunohistochemistry using a GFP antibody shows that most cones are GFP positive. (C) 4 weeks after subretinal injection, GFP transgene expression was most robust with the PR2.1 promoter, and GFP protein specifically located in L/M-cones (red) and visible as native fluorescence. (D) Wide field fundus photograph shows the posterior segment of a canine eye with the triangular shaped yellow-green tapetal fundus. It contains the round subretinal bleb superior to the optic nerve head visible immediately following successful injection. (E) Schematic representation of treated area in right eye 4 weeks after subretinal injection with PR2.1-GFP vector. The vector bleb (blue) is located within the canine tapetal fundus (green triangle) and covers part of the horizontally elongated area centralis (black), the site of maximal cone density. Robust GFP expression is visible without immunohistochemical enhancement in the center of the original subretinal vector bleb (E1). Transgene expression tapers off beyond the periphery of the bleb area (E2, E3). Calibration bars = 40  $\mu\text{m}$ .

**Figure 4.** Long-term restoration of cone retinal function after a single subretinal treatment with rAAV5-PR2.1-*hCNGB3*. (A) Representative 29-Hz cone flicker responses recorded from a

*CNGB3<sup>m/m</sup>*- and *CNGB3<sup>-/-</sup>*-mutant dog over 33 months after subretinal injection. The successful restoration of cone function was sustained in both animals without any long-term deterioration of the rescue effect. (B) Long-term restoration of the 29-Hz cone flicker responses are shown for 4 treated dogs (see also Table 1). There was no deterioration of the ERG amplitudes over time.

**Figure 5.** Restoration of day vision evaluated by objective behavioral testing with an obstacle avoidance course. The graph shows the transit time in seconds for dogs navigating a 3.6-m obstacle course as a function of ambient light intensity. *CNGB3<sup>m/m</sup>*- and *CNGB3<sup>-/-</sup>*-mutant animals were combined in this figure. Compared to untreated *CNGB3*-mutant dogs, transit times are significantly shorter in the unilaterally treated dogs at  $\geq 25$  lux. At higher light intensities of 65 and 646 lux, there were significant differences between the untreated and treated dogs, with the transit times in treated animals being close to the normal control values. Even though the transit time significantly improved with gene replacement therapy, it did not completely normalize, probably because only  $\sim 30\%$  of the retina was treated in only one eye. See Movie S2 (Supplementary Material) for examples of dogs navigating the obstacle avoidance course. Data of normal controls and untreated *CNGB3*-mutants taken from (42). P-values: \*  $p < 0.01$ ; \*\*  $p < 0.001$ ; \*\*\*  $p < 0.0001$ .

**Figure 6.** Restoration of normal protein localization following subretinal treatment with rAAV5-*hCNGB3* and rescue of cone function. Compared to the normal wildtype retina (A1, A3), both *alpha* transducin (GNAT2) and CNGA3 are not visible in the cone outer segments of the untreated canine *CNGB3<sup>-/-</sup>* (B1, B3) or *CNGB3<sup>m/m</sup>* (C1, C3) retinas. However, the localization of L/M-opsin is unaffected by disease (A2, A4, B2, B4, C2, C4). Normal cone outer segment

localization of both GNAT2 (D1, E1) and CNGA3 (D3, E3) was restored in vector treated regions of both the *CNGB3*<sup>-/-</sup> and *CNGB3*<sup>m/m</sup> retinas. Localization of L/M-opsin was unaffected by the treatment (D2, D4, E2, E4). Calibration bar = 20 μm. (F) Immunoblot of heterologously expressed CNGA3 subunits and canine retina homogenates using polyclonal anti-canine CNGA3-antibody. Despite the absence of CNGA3-labeling by immunohistochemistry in untreated *CNGB3*-mutant cones (B3, C3), a western blot shows that CNGA3 is present in both the canine *CNGB3*<sup>m/m</sup>- and *CNGB3*<sup>-/-</sup>- retinas. For comparison, cultured tSA-203 cells were transfected with canine *CNGA3* (right panel). The molecular weight of the major CNGA3 band is 103 kD; the faint band is 98 kD.

**Figure 7.** Representative histogram showing relative mRNA expression levels of the *hCNGB3* transgene as determined by qRT-PCR following subretinal injection with rAAV5-*hCNGB3*. (A) While no *hCNGB3* transgene expression was found in the wildtype (wt) and untreated achromatopsia (ACHM) retinas, all retinas injected with the therapeutic vector had detectable transgene expressions. The expression was highest with the PR2.1 promoter. The expression levels were significantly higher in the successfully PR2.1-injected retinas (with rescued cone function) compared to the non-successfully 3LCR-PR0.5-injected retinas (with no/transient rescue of cone function). For comparison expression levels of *L/M-*, *S-*, and *rod opsin* are shown. The expression levels of both *rod* and *cone opsins* are similar between wt and ACHM affected treated and untreated retinas. Only the *S-opsin* mRNA expression was significantly higher in the wt compared to the unsuccessfully treated ACHM retinas. P-values: \* p<0.05. (B) For comparison, a scatter plot shows the expression levels of the cone-specific genes *cCNGA3*, *cCNGB3*, *L/M-*, and *S-opsin* in untreated normal wildtype (wt, n=7), carrier (*CNGB3*<sup>+m</sup>, n=3;

*CNGB3*<sup>+/-</sup>, n=4), and ACHM-affected dogs (*CNGB3*<sup>m/m</sup>, n=3; *CNGB3*<sup>-/-</sup>, n=3). Except for the non-detectable *cCNGB3* in the *CNGB3*<sup>-/-</sup> dogs, the expression levels did not differ between animal groups. (C) Cone ERG flicker amplitude increased with higher *hCNGB3* transgene expression: Comparison of detectable retinal *hCNGB3* transgene expression levels with the cone flicker ERG amplitudes measured before tissue collection in 12 eyes revealed a highly significant nonparametric Spearman rank correlation of 0.85 (p<0.0001).

Relative gene expression for each gene compared to 18S was calculated as  $1 / [2^{-(Ct_{\text{Gene}} - Ct_{18S})}]$ .



## TABLES

**Table 1.** Eyes injected subretinally with rAAV5-*GFP* or rAAV5-*hCNGB3*.

Promoter / Vector Construct	Dog ID / Gender	Eye	Age at Tx (weeks)	Vol (μL)	Conc (vg·mL <sup>-1</sup> )	Studies & Gene Expression Longest Follow-up Period (weeks)			
						ERG	Obstacle	Morphology / IHC	qRT-PCR
<b>PR0.5-<i>hCNGB3</i></b>	M577/m	L	4	60	1.53 x 10 <sup>14</sup>	11		33	
	GS80/m	L	8	70	1.53 x 10 <sup>14</sup>	39	56	74	
<b>3LCR-PR0.5-<i>GFP</i></b>	M582/m	R	7	110	2.55 x 10 <sup>12</sup>	10		25	
	M583/m	R	7	110	2.55 x 10 <sup>12</sup>	31		38	
<b>3LCR-PR0.5- <i>hCNGB3</i></b>	M583/m	L	7	110	7.48 x 10 <sup>12</sup>	4		39	
	GS89/f	L	8	110	7.48 x 10 <sup>12</sup>	115			115
	M608/m	L	9	120	1.73 x 10 <sup>12</sup>	3		5	
	M596/f	R	23	140	5.28 x 10 <sup>12</sup>	37			37
	M574/f	L	28	110	2.05 x 10 <sup>12</sup>	31			88
	M589/m	R	60	140	5.28 x 10 <sup>12</sup>	34			36
	M575/f	R	81	120	1.73 x 10 <sup>12</sup>	30			38
<b>PR2.1-<i>GFP</i></b>	M570/m	L	6	80	8 x 10 <sup>14</sup>			4	
	M573/f	L	3	90	1.36 x 10 <sup>13</sup>			4	
<b>PR2.1-<i>hCNGB3</i></b>	M606/m	R	3	120	9.43 x 10 <sup>12</sup>	27			41
	GS118/f	L	7	130	8.47 x 10 <sup>10</sup>	27		28	
	GS94/m	L	10	80	7.23 x 10 <sup>12</sup>	130	42		
	M598/m	L	11	110	4.33 x 10 <sup>12</sup>	48			48
		R	11	130	4.33 x 10 <sup>12</sup>	48			48
	GS99/f	L	12	120	1.29 x 10 <sup>13</sup>	45			45
	M625/m	R	12	110	9.39 x 10 <sup>12</sup>	9		12	
	M617/m	R	13	110	1.65 x 10 <sup>13</sup>	45			
	M584/m	L	14	180	7.23 x 10 <sup>12</sup>	130	42		
	M625/m	L	17	150	8.67 x 10 <sup>12</sup>	4		7	
	M626/m	L	17	190	8.67 x 10 <sup>12</sup>	9	8		26
		R	17	190	8.67 x 10 <sup>12</sup>	9	8		26
	M627/m	L	17	140	6.50 x 10 <sup>12</sup>	4	5		26
		R	17	140	8.67 x 10 <sup>12</sup>	4	5		26
	GS87/m	R	54	150	7.73 x 10 <sup>12</sup>	44			44
	GS89/f	R	54	150	7.73 x 10 <sup>12</sup>	68			68
GS80/m	L	66	160	7.28 x 10 <sup>12</sup>	4		16		

All dogs with M prefix in ID are Alaskan Malamute-derived and are homozygous for the genomic deletion of *CNGB3* (*CNGB3*<sup>-/-</sup>). All dogs with the GS prefix are derived from German Shorthaired Pointer and are homozygous for the D262N missense mutation of *CNGB3* (*CNGB3*<sup>m/m</sup>).

**Table 2.** Summary of treatment outcome as a function of vector promoter and age of dogs.

	Treatment outcome (Rescue of cone function)	# Eyes		
		PR0.5	3LCR-PR0.5	PR2.1
Human red cone opsin promoter				
<b>Younger dogs (<math>\leq 28</math> weeks)</b>	No response	1	3	3
	Transient response	1	2	0
	Sustained response	0	0	11
<b>Older dogs (<math>\geq 54</math> weeks)</b>	No response	-	2	2
	Transient response	-	0	0
	Sustained response	-	0	1

## FIGURES

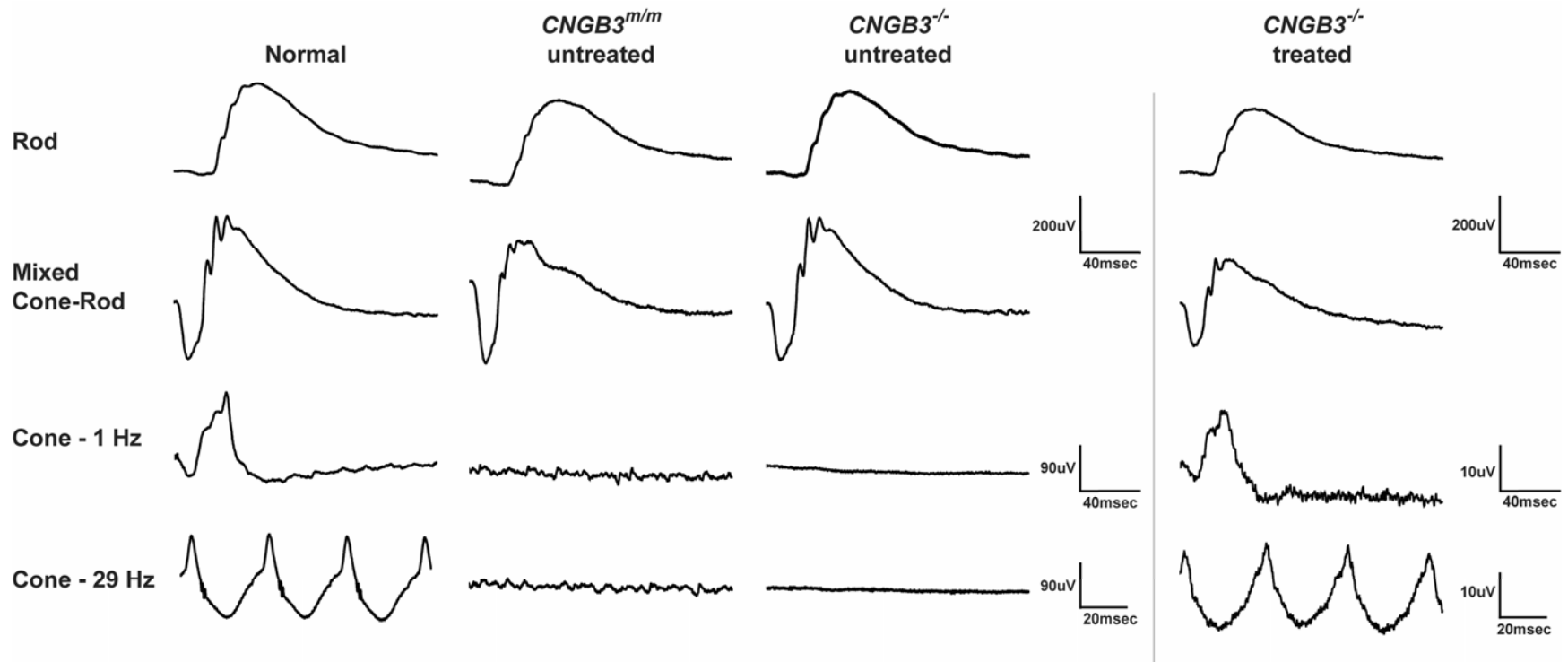


Figure 1.

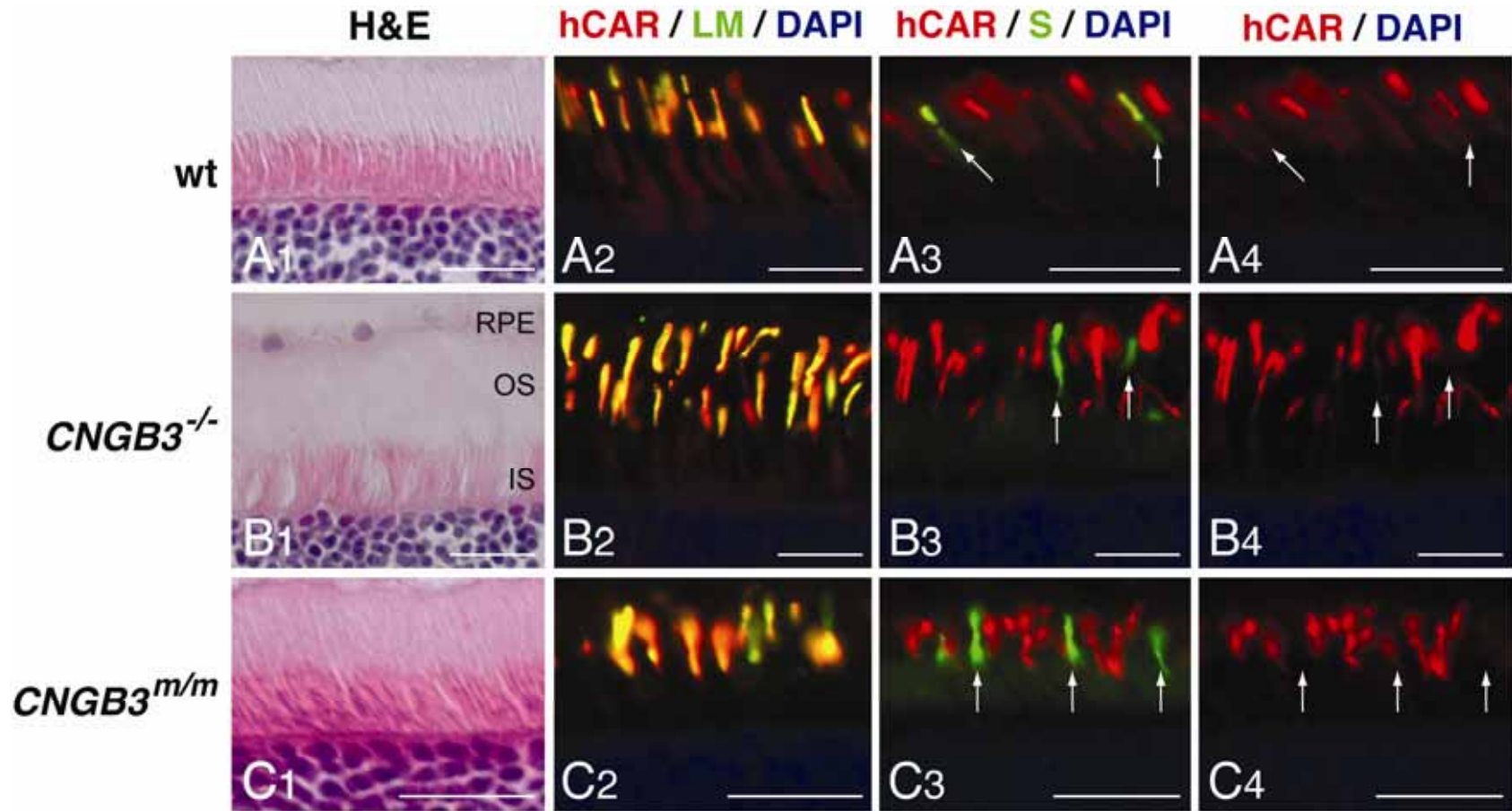


Figure 2.

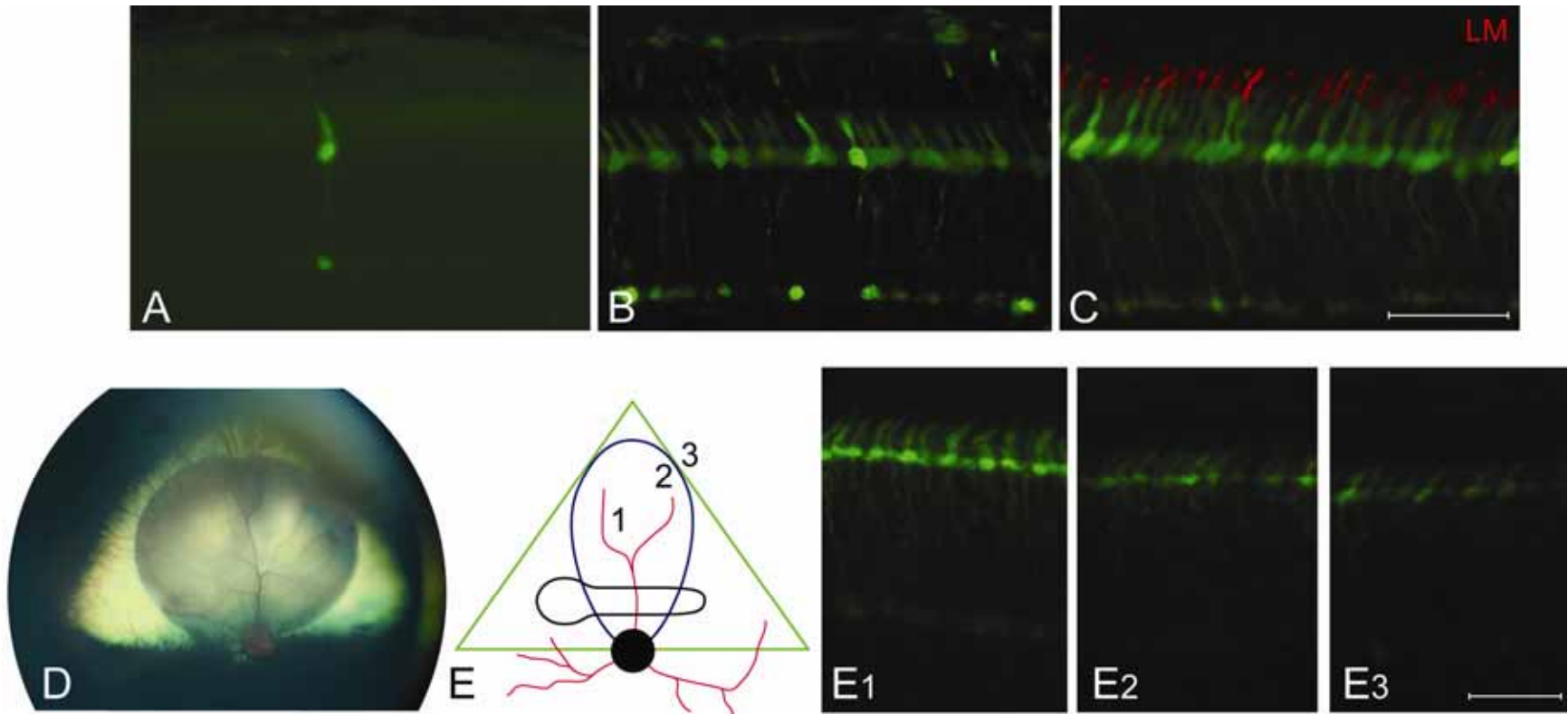


Figure 3.

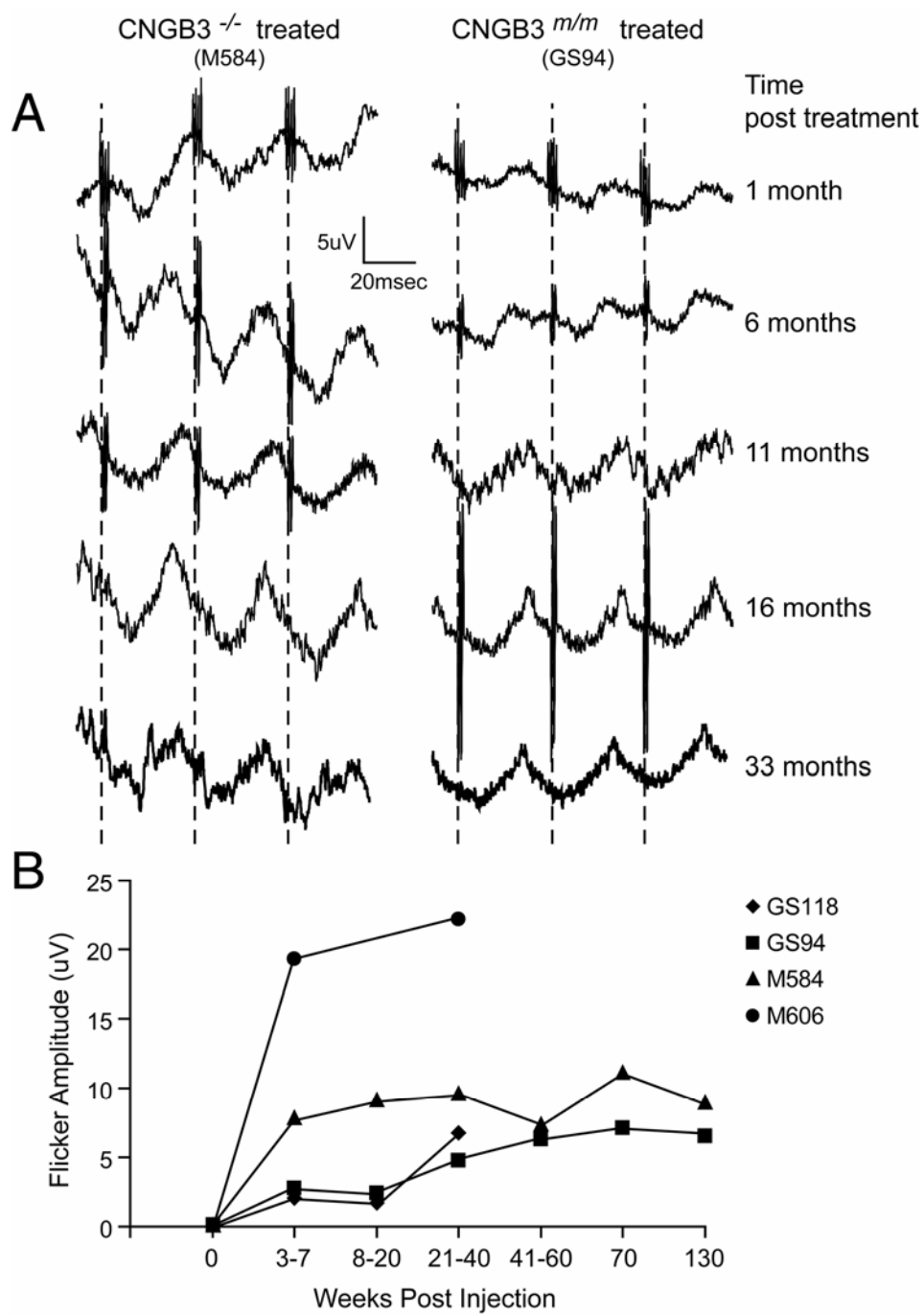


Figure 4.

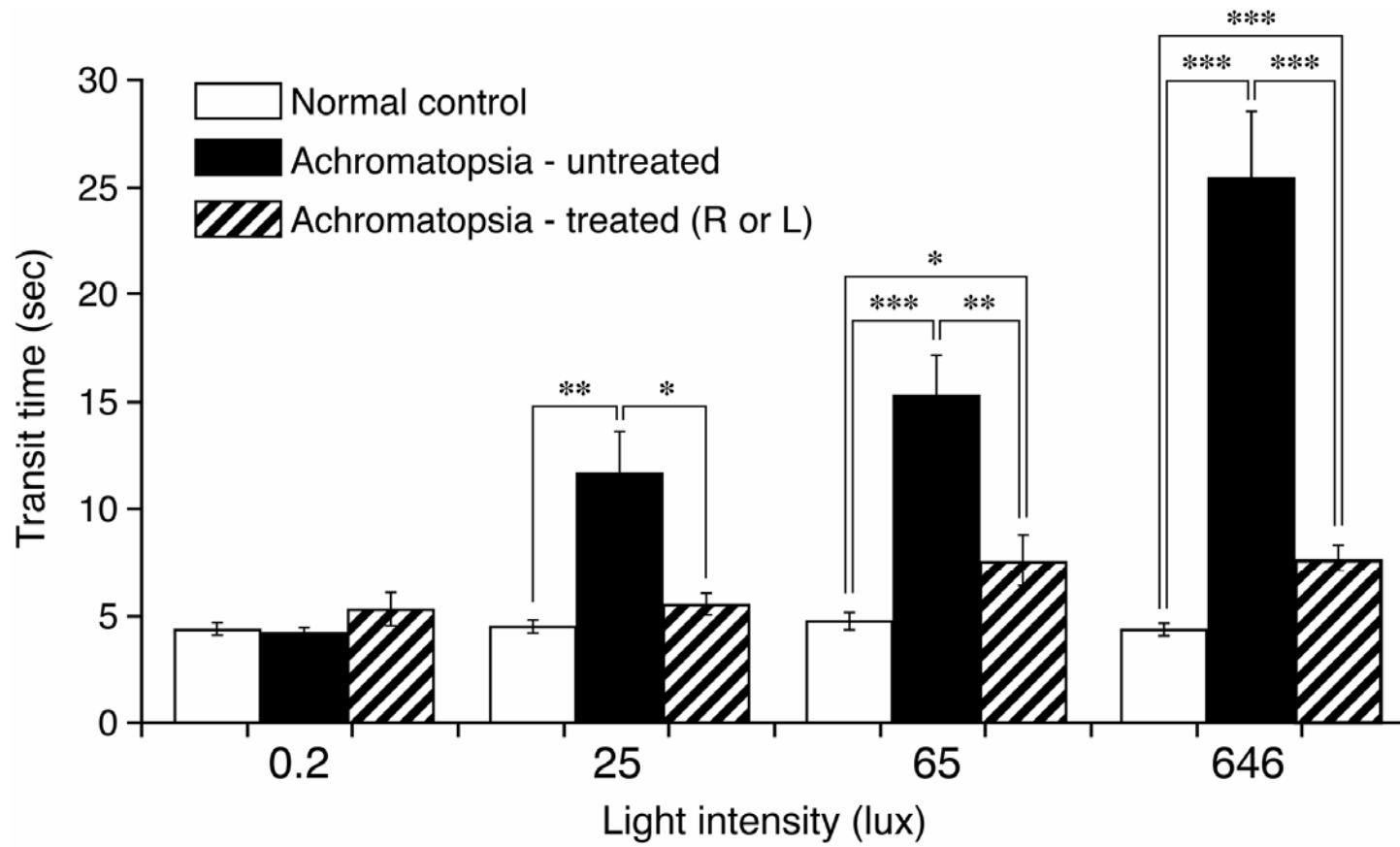


Figure 5.



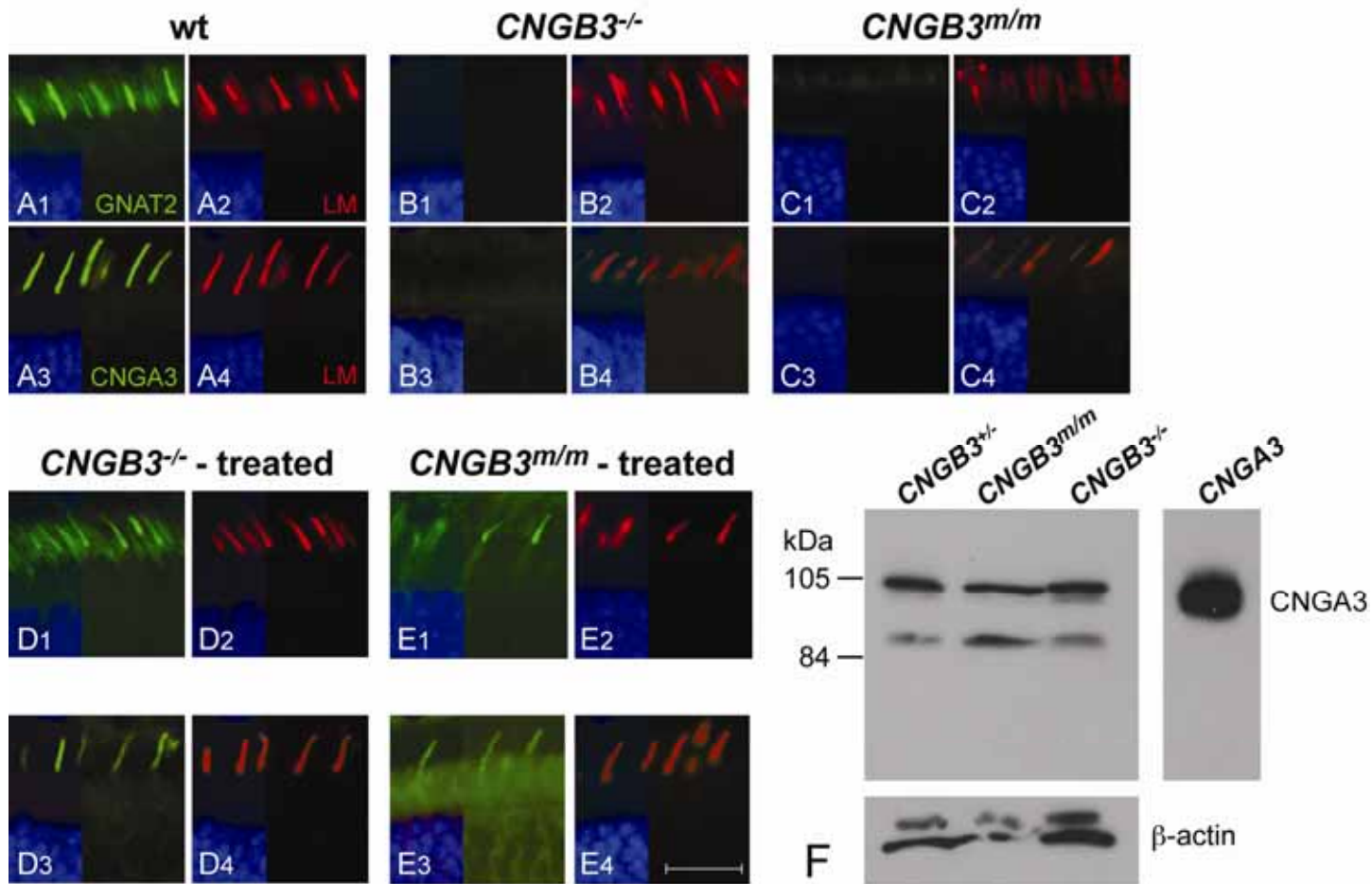


Figure 6.

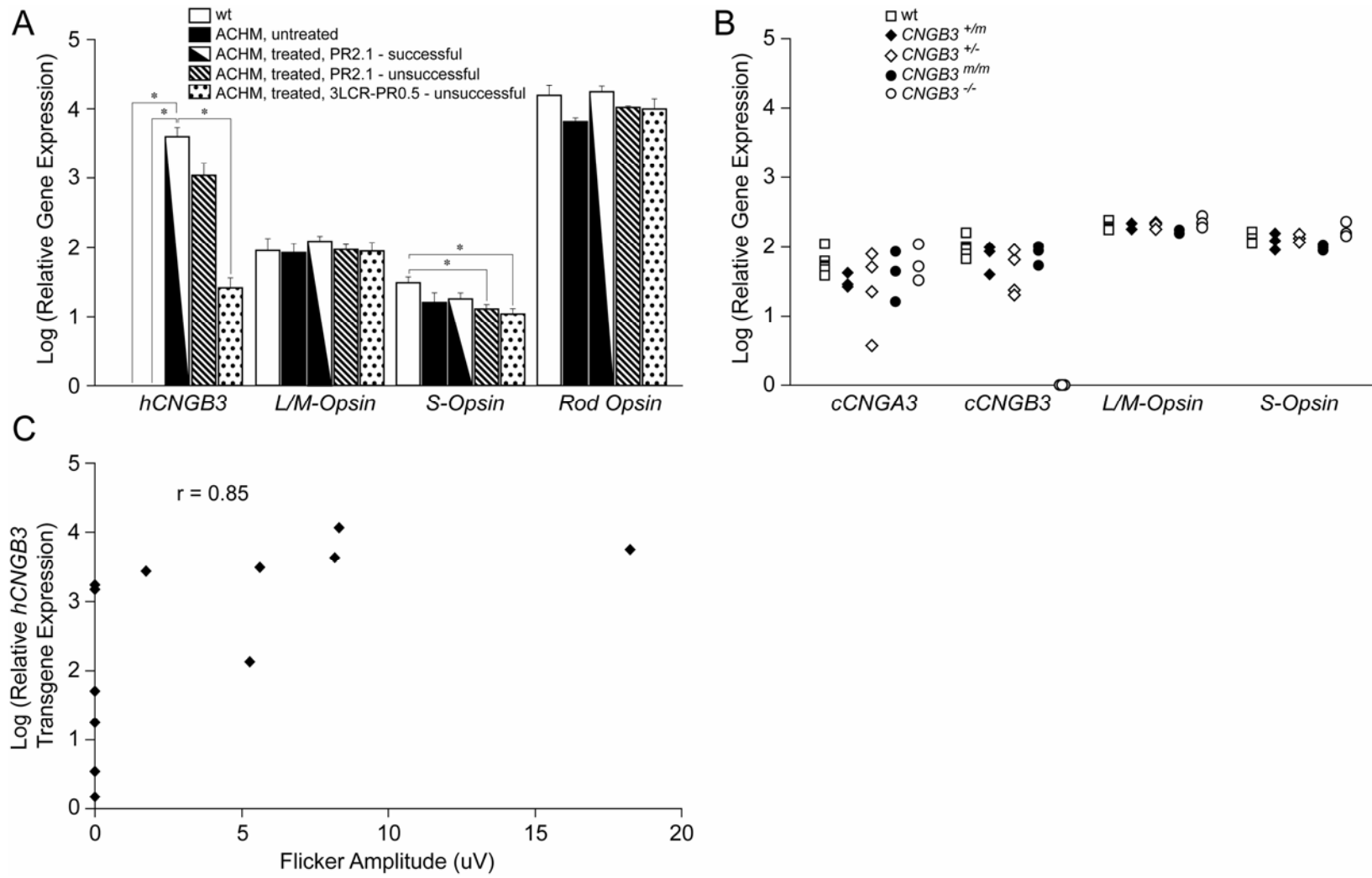


Figure 7.

## ABBREVIATIONS

AAV, adeno-associated virus; ACHM, achromatopsia; CNG, cyclic nucleotide-gated channel; CNGA3, *alpha* subunit of the cone cyclic nucleotide gated channel; CNGB3, *beta* subunit of the cone cyclic nucleotide gated channel; CPFL, cone photoreceptor function loss; ERG, electroretinogram; GNAT2, *alpha* subunit of cone transducin; hCAR, human cone arrestin; LCA, Leber Congenital Amaurosis; LCR, locus control region; L/M, long/medium-wavelength-absorbing; PDE6B, rod cGMP-phosphodiesterase *beta*-subunit; PR, promoter; qRT-PCR, quantitative real-time PCR; rAAV, recombinant AAV; RPE, retinal pigment epithelium; RPE65, RPE-specific protein 65kDa; S, short-wavelength-absorbing.